Journal Name

ARTICLE

Supplementary Information

A high-rate aqueous rechargeable zinc ion battery based on VS_4@rGO nanocomposite

Haigang Qin,[ab] Zhanhong Yang,[*a] Linlin Chen,[ab] Xi Chen,[ab] and Limin Wang[ab]

[a]Hunan Province Key Laboratory of Chemical Power Source, College of Chemistry and Chemical Engineering, Central South University, Changsha 410083, China.

[b]Innovation Base of Energy and Chemical Materials for Graduate Students Training, Central South University, Changsha 410083, China.

*Correspondence to:

Prof. Zhanhong Yang, Email: zhyang@csu.edu.cn

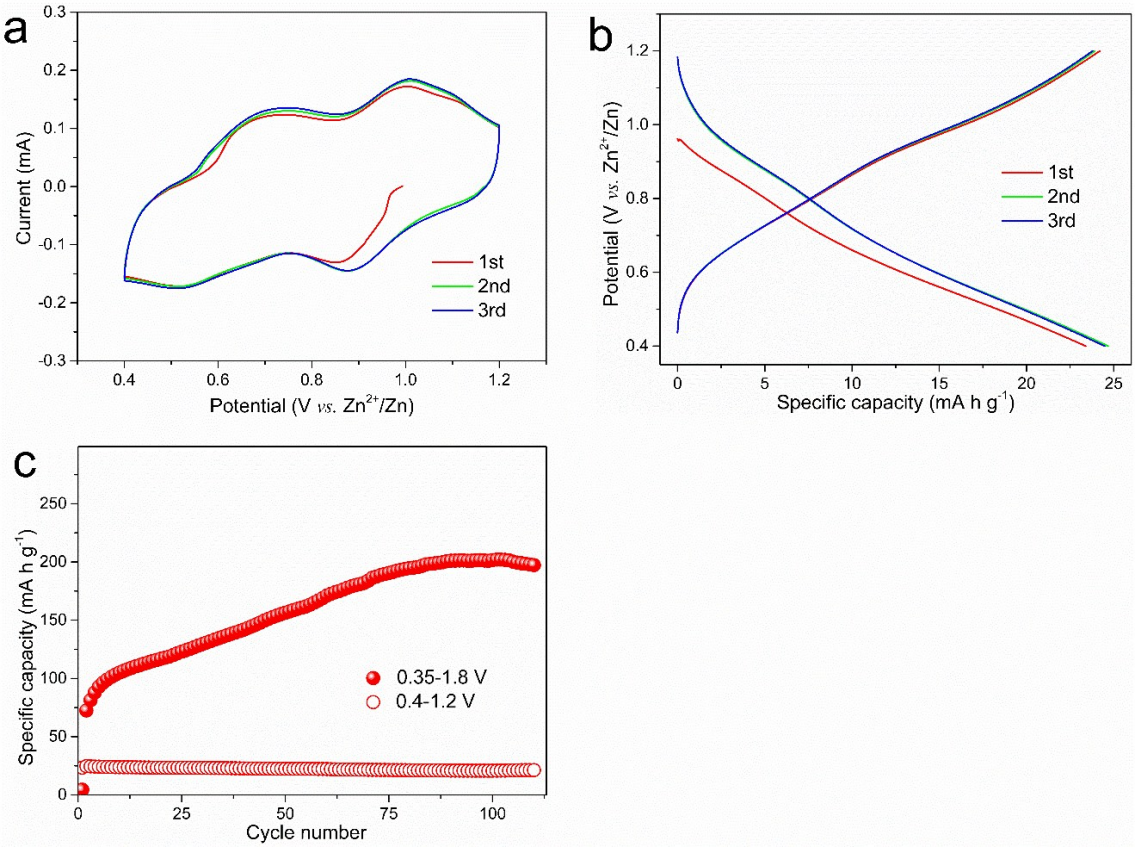

Figure S1. Electrochemical performances of VS_4@rGO at the voltage range of 0.4 to 1.2 V. (a) CV curves at 0.5 mV s^{-1}. (b) Discharge-charge curves at 0.2 A g^{-1}. (c) Cycle performance at 0.2 A g^{-1}, compared with that of 0.35 to 1.8 V.

Table S1. Contribution of the charge capacity between 1.4 V and 1.8 V to the total charge capacity and the Coulombic efficiency at different current density in Fig. 4e

Current density (A/g)	0.2	0.5	0.8	1	2

Charge capacity (1.4 to 1.8 V)/total charge capacity	27.8%	17.3%	12.5%	11.1%	8.9%
Coulombic efficiency	89.3%	94.1%	96.9%	97.6%	99%

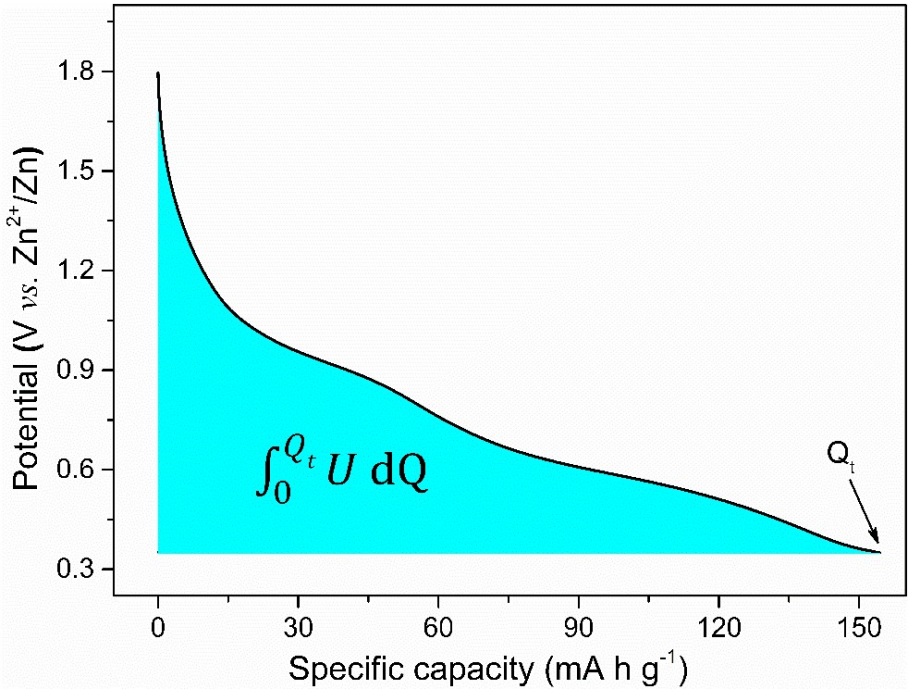

Figure S2. Discharge curve at 0.1 A g^{-1}.

The average discharge voltage is calculated as follow:

$$\bar{U} = \frac{1}{Qt}\int_{0}^{Qt} U\, dQ$$

where U and Q are the voltage and the discharge capacity respectively, and Q_t is the total capacity.

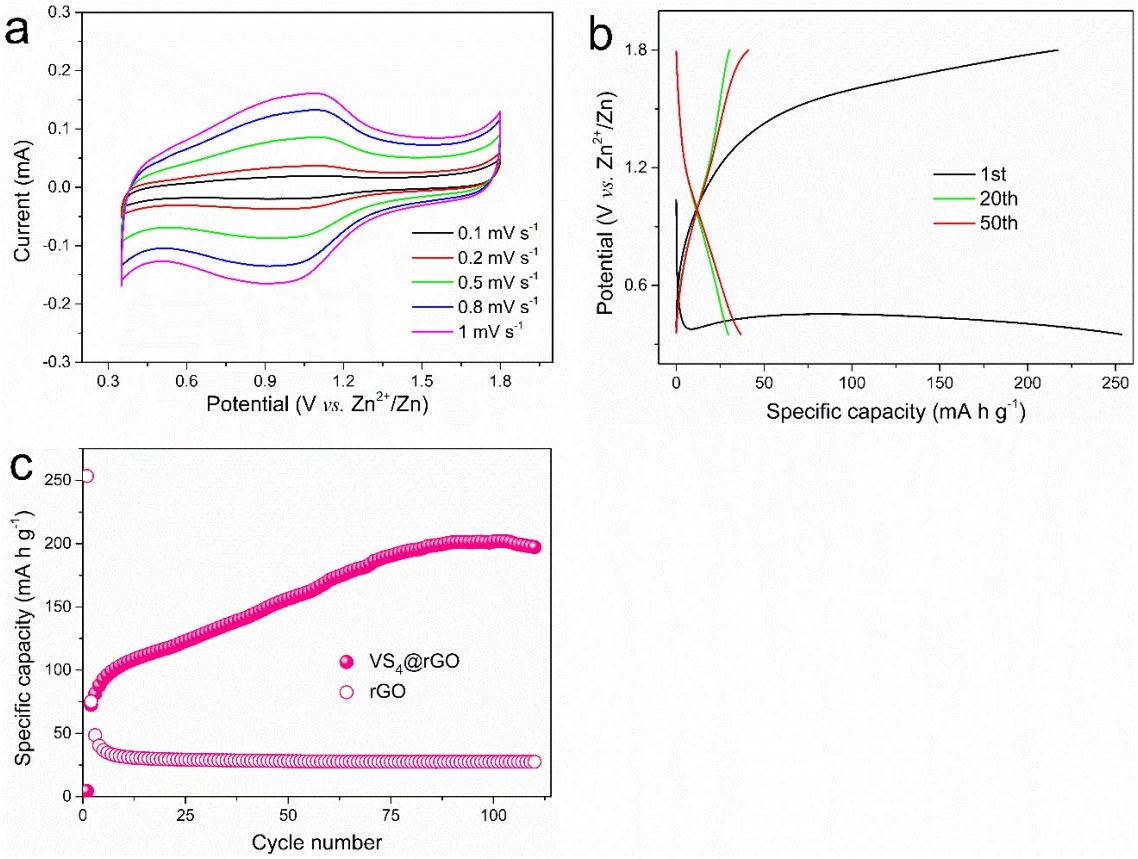

Figure S3. Electrochemical performances of rGO. (a) CV curves at 0.1, 0.2, 0.3, 0.5, 0.8 and 1 mV s^{-1}. (b) Discharge-charge curves at 0.2 A g^{-1}. (c) Cycle performance at 0.2 A g^{-1}, compared with that of VS_4@rGO.

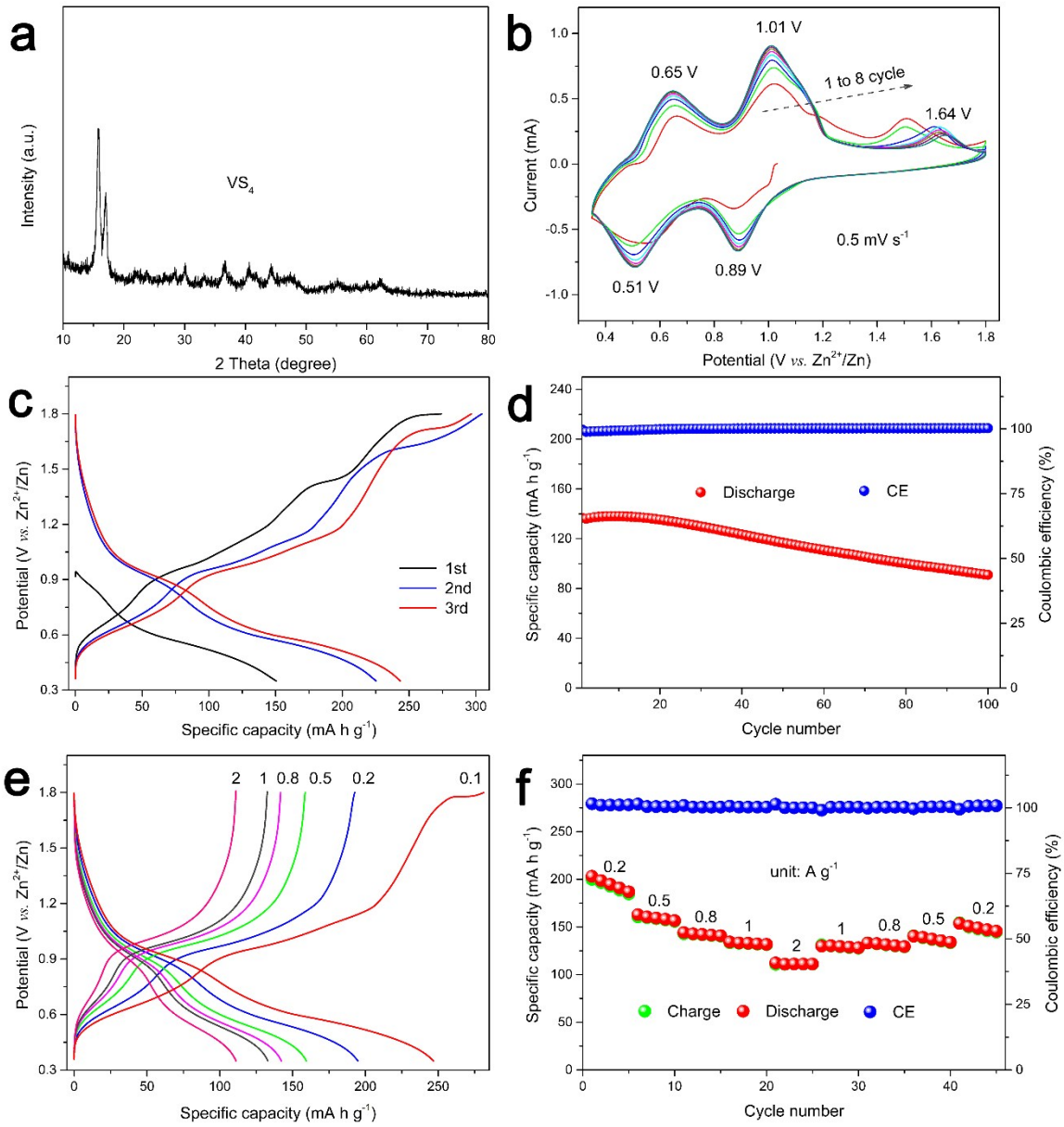

Figure S4. (a) XRD pattern of VS_4. Electrochemical performances of VS_4, (b) CV curves at 0.5 mV s^{-1}; (c) charge-discharge curves at 0.1 A g^{-1}; (d) cycle performance at 1 A g^{-1}; (e) charge-discharge profiles at 0.1, 0.2, 0.5, 0.8, 1 and 2 A g^{-1}; (f) rate performance.

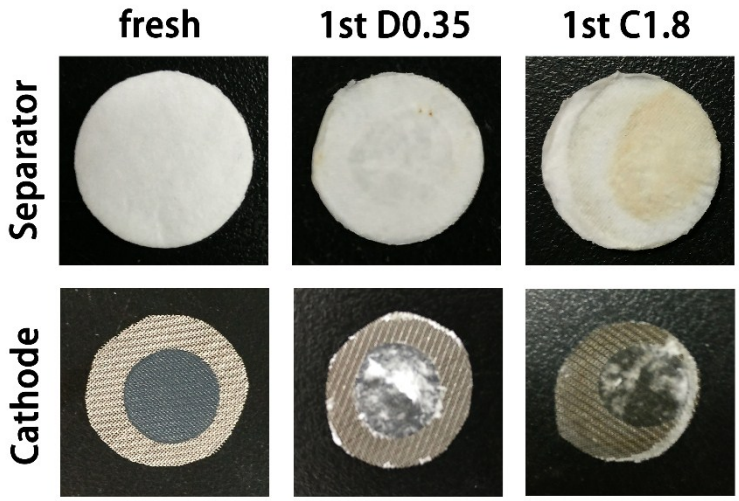

Figure S5. Digital photographs of separators (the side facing cathode) and the corresponding cathodes from disassembled CR2025-type coin cells in the full discharge (1st D0.35) and full charge (1st C1.8) states of the first cycle. The white fiber on the cathode came from the separator, which was caused by the disassembled process. The yellow color on the separator of 1st C1.8 appears roughly in the area where has a direct contact with electrode materials.

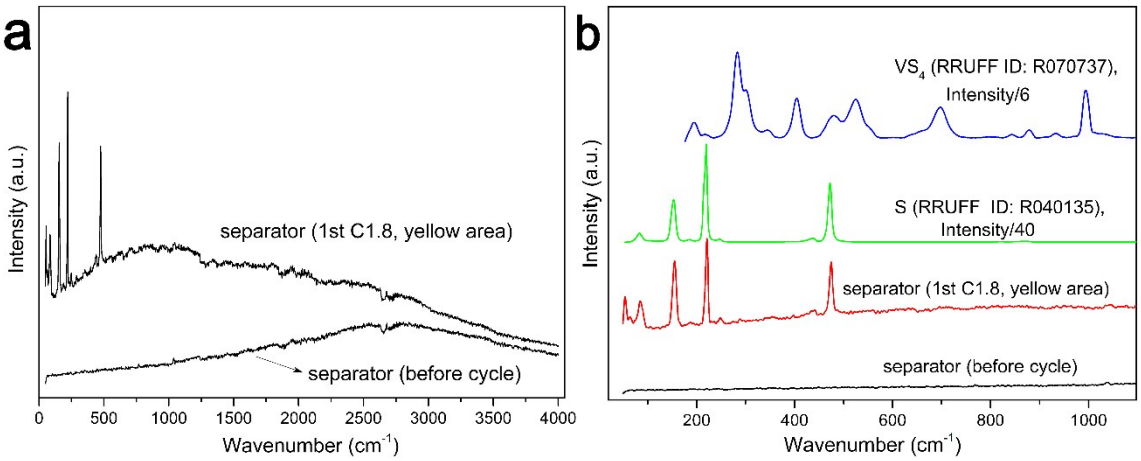

Figure S6. (a) Raman spectra of separators before cycle and in the full charge state of the first cycle (the test sample was taken from the yellow area). (b) Raman spectra of separators at the wavenumber range from 50 to 1100 cm^{-1} (black curve and red curve). The green curve and the blue curve are the Raman spectra of sulfur and patronite in the RRUFF database, respectively. The Raman peaks of sulfur appeared at the Raman spectrum of the separator in full charge state of the first cycle reveals that the sulfur is the composition of the yellow chemicals.

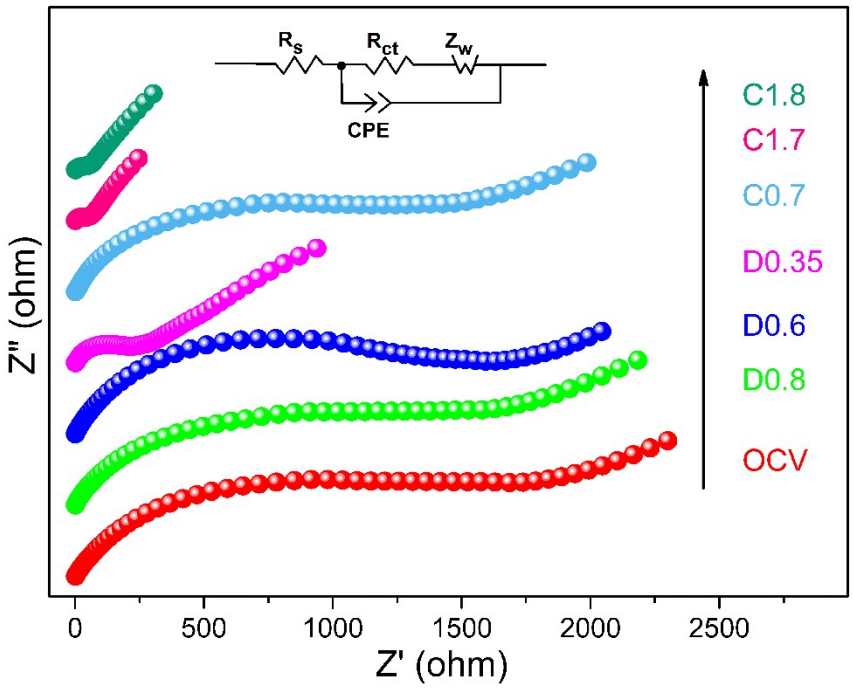

Figure S7. EIS results at different states of the first discharge-charge process; inset shows the equivalent circuit.

Table S2. Fitting Rs and Rct values of Nyquist plots in Figure S7

State	OCV	D0.8	D0.6	D0.35	C0.7	C1.7	C1.8
$R_s(\Omega)$	1.49	1.22	1.19	1.21	1.15	1.56	1.73
$R_{ct}(\Omega)$	650	523	497	223	517	60.8	75.2

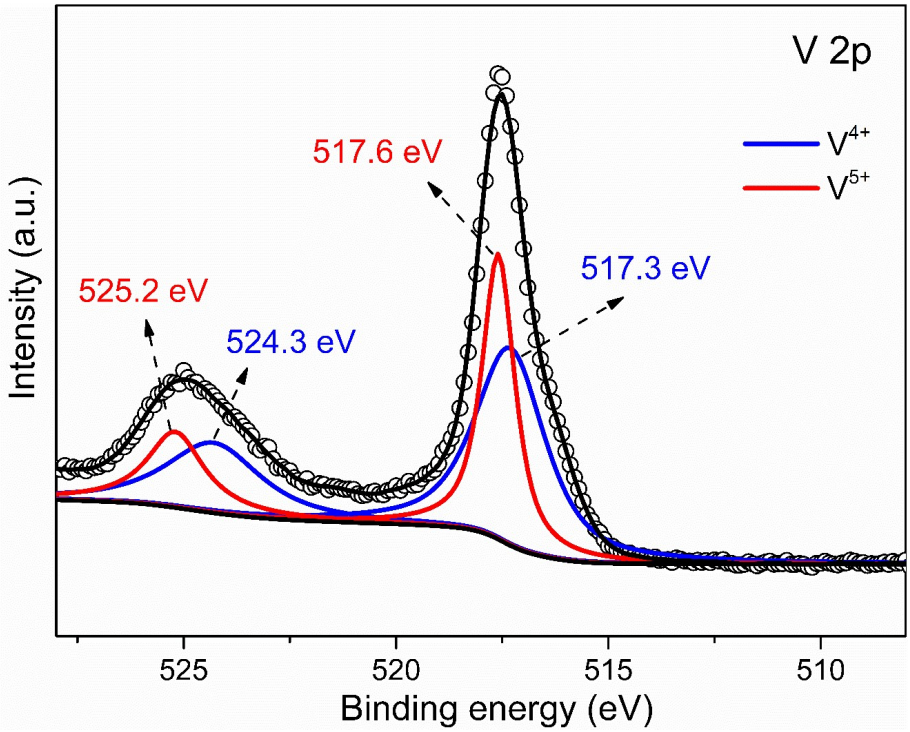

Figure S8. XPS spectrum of V 2p core level at full charge state of the third discharge-charge cycle.

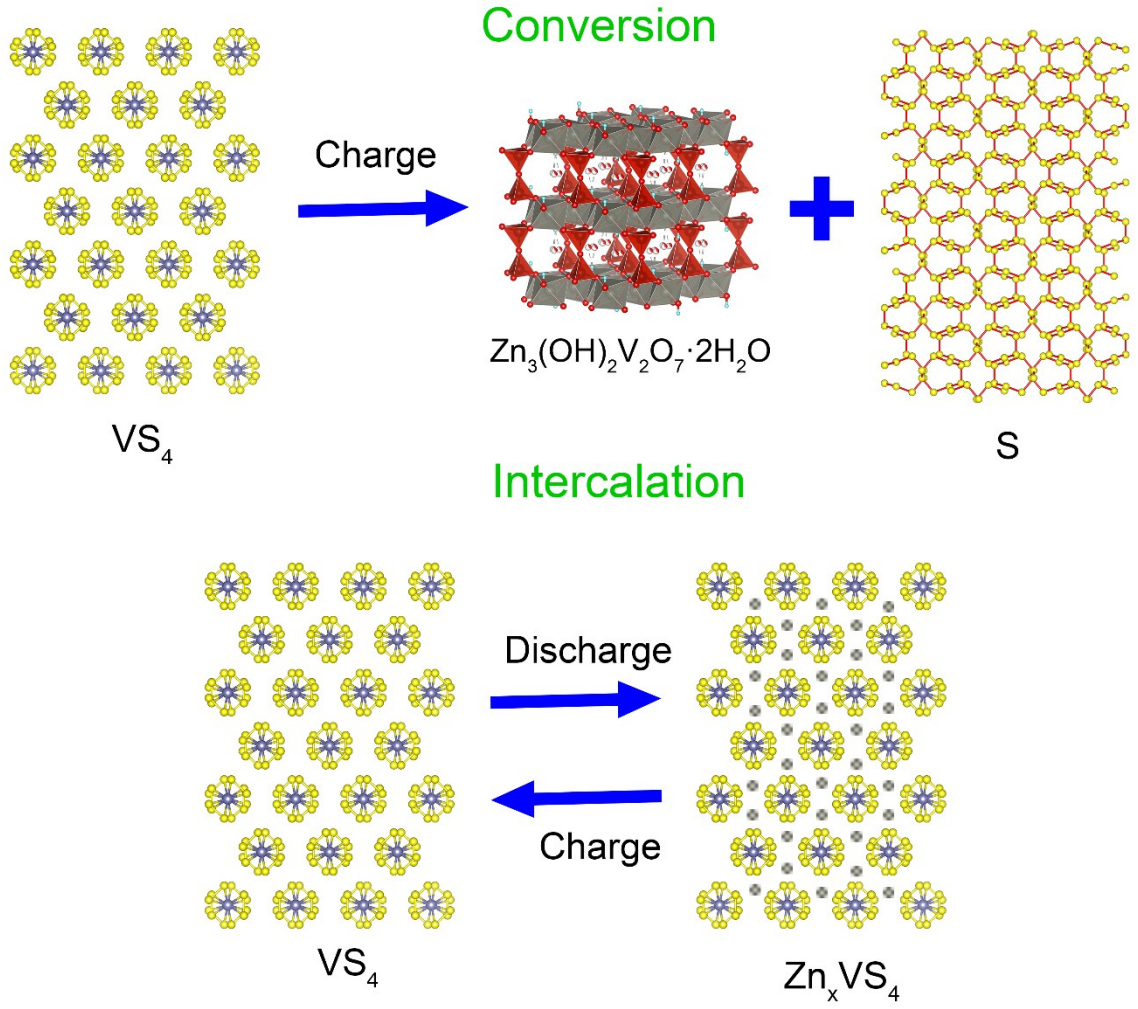

Figure S9. Schematic illustration for the partial reaction mechanism of VS_4@rGO during the third cycle.